

B. VINCENT<sup>1,\*</sup>  
R. KREMER<sup>1</sup>  
A. BOUDRIOUA<sup>1,✉,\*\*</sup>  
P. MORETTI<sup>2</sup>  
Y.-C. ZHANG<sup>3</sup>  
C.-C. HSU<sup>3</sup>  
L.-H. PENG<sup>3</sup>

# Green light generation in a periodically poled Zn-doped LiNbO<sub>3</sub> planar waveguide fabricated by He<sup>+</sup> implantation

<sup>1</sup> Laboratoire Matériaux Optiques, Photonique et Systèmes, Unité Mixte de Recherche (UMR), Centre National de la Recherche Scientifique (CNRS), UMR 7132, Université de Metz et Supélec, 8 rue E. Belin, 57070 Metz, France

<sup>2</sup> Laboratoire de Physico-chimie des Matériaux Luminescents, Unité Mixte de Recherche (UMR), Centre National de la Recherche Scientifique (CNRS), No. 5620, Université Claude Bernard, Lyon I, France

<sup>3</sup> Institute of Electro-Optical Engineering and Department of Electrical Engineering, National Taiwan University, Taipei 106, Taiwan, R.O.C.

Received: 26 January 2007/Revised version: 2 September 2007  
Published online: 29 September 2007 • © Springer-Verlag 2007

**ABSTRACT** An optical planar waveguide is investigated in ZnO-doped periodically poled lithium niobate formed by He<sup>+</sup> implantation. Optical losses were found to be 2 dB/cm. Second-harmonic generation is used to produce a green laser beam by quasi-phase matching in the obtained waveguide. The conversion efficiency was found to be 10<sup>-2</sup>%/W. Photorefractive resistance properties are reported and discussed relating to undoped periodically poled lithium niobate.

PACS 42.65.-k; 42.65.Wi; 42.82.-m

## 1 Introduction

Periodically poled lithium niobate (PPLN) structures with KNbO<sub>3</sub> and KTiOPO<sub>4</sub> are one of the most promising components for frequency doubling and therefore for the realization of visible laser sources at short wavelengths [1–4]. However, LiNbO<sub>3</sub> is known to have high photorefractive properties, i.e. index variation when illuminated by high laser power density [5, 6]. That effect induces a degradation of the beam shape and affects the quasi-phase-matching (QPM) conditions. As a whole, second harmonic generation (SHG) power decreases and the stability of laser sources is substantially affected. In nonlinear optics, where the main goal is to preserve a beam of high quality, the photorefractive phenomenon appears rather as an adverse effect. It is important to note that the photorefractive effect, based on the photo-excitation of impurities present in the crystal, is more important with short wavelengths. That is why this phenomenon is more critical for frequency doubling than for optical parametric oscillation applications. The origin of this effect is well studied in monodomain LiNbO<sub>3</sub> and also in PPLN crystals [7, 8]. As a matter of fact, the photorefractive effect is due

to the electro-optic effect induced by the electric field resulting from charge displacement within the material due to light absorption.

A solution to avoid this effect is to increase the intrinsic conductivity of the material (without illumination) by doping it for example with MgO and/or to increase the temperature of the crystal [9]. Another alternative is to balance the ratio of Fe<sup>2+</sup> and Fe<sup>3+</sup>, which is particularly true for the case where the current diffusion is more important. This phenomenon has been reported by different authors [10, 11]. For instance, it was shown that the photorefractive properties of Fe-doped materials can be varied over a wide range by changing the reduction ratio through proton irradiation of the sample. In the case of PPLN, this effect is somehow different because the sign of the photovoltaic current, i.e. the resulting space-charge field along the optical *C* axis, changes periodically within the domains. For instance, Sturman et al. [12] proposed a model to connect the photorefractive effect with the grating period ( $\Lambda$ ) and the Gaussian beam dimensions. When the size of the beam (the waist  $W_0$ ) is large compared to the period of the QPM grating, it can have a compensation for the accumulated charges on the edge of the beam. In this case the electric field is localized on the edge of the beam and its transverse components as well as the change of the extraordinary refractive index are weak. It is thus understood that the photorefractive effect is weaker in a PPLN crystal than in monodomain LiNbO<sub>3</sub> crystals. In addition to that, it was shown that the ratio  $\Delta n_{\text{PPLN}}/\Delta n_{\text{LN}}$  is proportional to the square of the ratio  $\Lambda/2W_0$  [13].

Up to now, LiNbO<sub>3</sub>:MgO is the only doped LiNbO<sub>3</sub> commercially available because the Czochralsky growth technique [14, 15] is difficult to carry on when a proportion of impurity has to be maintained constant in the whole crystal. The use of MgO was extensively studied for its ability to reduce the optical damage due to the photorefractive effect. It was shown that a proportion of 5% of MgO can substantially increase the optical threshold (intensity of SHG of a Nd:YAG laser beyond which the beam is deformed along the *C* axis of the crystal for an exposure of 10 nm) [16], whereas 1.8% of MgO is sufficient in the stoichiometric LiNbO<sub>3</sub> [17].

However, MgO is far from being perfect for LiNbO<sub>3</sub> doping, especially for QPM applications. Firstly, when it is illu-

✉ Fax: +33-149403400, E-mail: boudrioua@galilee.univ-paris13.fr

\*Currently at: Laboratoire de Physique des Milieux Ionisés et Applications, Unité Mixte de Recherche (UMR), Centre National de la Recherche Scientifique (CNRS), No. 7040, Université de Henri Poincaré, Nancy I, France

\*\*Present address: LPL, Institut Galilée, Université Paris 13, France

minated with strong fluences, color centers are created and, secondly, during the poling process, the transverse velocity of the domain wall is increased, which implies a complicated technological process to realize short-period PPLN structures ( $< 10 \mu\text{m}$ ). This is particularly true in order to obtain a thick PPLN sample as the domain width increases beneath the electrodes throughout the crystal thickness. More details of this phenomenon are reported in [18]. For all these reasons, more recently, many researchers have tried to find other doping components that could be built in in the matrix of  $\text{LiNbO}_3$ . Volk et al. [19] suggested that doping by ZnO could be a good response to the problems caused by the use of MgO. During the growth by the Czochralsky method, ZnO can be added to the growth bath. Peng et al. [20] showed that it was possible to cause a significant drop in the coercive field and simultaneously to maintain an accurate control of the domain propagation by using ZnO as doping agent in the matrix of  $\text{LiNbO}_3$ .

In this study, our main objective consists of combining, for the first time to the best of our knowledge, the utilization of ionic implantation with periodically poled ZnO-doped lithium niobate (PPZnLN) structures to fabricate waveguides for efficient second-harmonic generation (SHG) of a Nd:YAG laser beam. Light-ion implantation has been extensively studied in order to produce waveguides in various nonlinear materials [21]. Moreover, it has been demonstrated that this technique preserves the linear and the nonlinear optical properties of the guiding region of monodomain  $\text{LiNbO}_3$  [22] as well as the periodically poled  $\text{LiNbO}_3$  (PPLN) [23]. Note that contradictory results have also been reported, indicating that the two-wave-mixing properties are strongly affected by ion implantation (time response, direction of the energy exchange, strength of the wave coupling, wave coupling by the photovoltaic effect in unexpected configurations, and so on). Thus, all the coefficients (electro-optic, photovoltaic, nonlinear) are modified [24–26]. Results of the investigation of SHG of a green laser will be reported and discussed. The issue of resistance to the optical damage will also be reported.

## 2 Sample preparation

### 2.1 PPLN fabrication

In order to fabricate PPLN structures, different techniques have been studied such as electron-beam scanning, Ti in-diffusion, ionic exchange or electric field poling [27, 28]. The methods based on ion exchange or in-diffusion are limited by the depth of the domain inversion and by the domain shape, which can be triangular (Ti in-diffusion,  $\text{Li}_2\text{O}$  out-diffusion) or semicircular (proton exchange followed by heat treatment) giving a non-optimized grating for frequency conversion. Conversely, electric field poling gives domains with straight walls, which is the best geometry suitable for SHG [29].

For this work, we used  $z$ -cut PPLN samples of  $5 \times 6 \times 0.33 \text{ mm}^3$  Zn doped at 6 mol. % with a grating period of  $6.7 \mu\text{m}$  (along the  $y$  axis). The latter are suitable for frequency doubling of a Nd:YAG laser beam by using first-order quasi-phase matching at  $60^\circ\text{C}$  and  $23^\circ\text{C}$  in bulk interactions. Single-domain lithium niobate crystal homogeneously doped with ZnO (6%) was obtained by the Czochralsky technique. Afterwards, the crystal was poled by electric field poling of

$2.5 \text{ kV/mm}$  at room temperature. For that, the sample was patterned by standard UV photolithography with photoresist polymer and then placed in a cell with liquid electrodes.

### 2.2 Waveguide fabrication

We chose to fabricate a waveguide with a maximum thickness in order to be able to easily couple maximum power into the waveguide. For that, we used triple  $\text{He}^+$  implantation with energies of 1.8, 1.9 and 2 MeV, which is the maximum value that can be reached with our Van der Graaf accelerator. For each implantation, the dose was  $0.5 \times 10^{16} \text{ ions/cm}^2$  in order to produce an important index variation in the barrier ( $\sim 2 \times 10^{-2}$ ) [21] and thus to obtain a strong light confinement. For the same purpose, a triple implantation allowed us to enlarge the optical barrier and thus to reduce optical losses by the tunneling effect [30].

The ionic implantation induces a refractive-index change by electronic defects in the guiding region and by nuclear defects at the end of their path in the region we called the optical barrier. The electronic defects cause only a slight index variation ( $\sim 0.001$ ) but the nuclear defects involve a decrease in the refractive index of 0.02 depending on the material and the implantation parameters used. In lithium niobate the ordinary index and the extraordinary one undergo changes of their values. Recently, we have also demonstrated that PPLN structures undergo the same effects [23]. A thermal annealing procedure of 1 h at  $200^\circ\text{C}$  was applied after the waveguide realization in order to reduce defects in the guiding region.

## 3 Results and discussion

### 3.1 Linear optical characterization

This study is of twofold interest: it emphasizes the feasibility of waveguides in Zn-doped PPLN crystal by  $\text{He}^+$  implantation and it allows analyzing the variation of refractive indices according to the wavelength.

The effective indices were measured by using dark  $m$ -lines spectroscopy [31] and their comparisons with those calculated for a step-like waveguide give the guide parameters, namely  $n_o = 2.286$ ,  $n_e = 2.206$  and a thickness  $t = 3.3 \mu\text{m}$ . The good correlation between these two sets of values allows us to establish that our guide has a step-like index, which is confirmed by the reconstruction of index profiles by the  $i$ -WKB (Wentzel–Kramers–Brillouin) method [32, 33] as displayed in Fig. 1.

We carried out the same measurements with several wavelengths in order to determine the variation of the refractive indices according to the wavelength. These measurements are of particular interest since Sellmeier equations of Zn-doped lithium niobate differ according to various authors. Figure 2 presents the chromatic dispersion of the guiding region for both ordinary and extraordinary indices at room temperature. These experimental values were adjusted with the following Sellmeier equation:

$$n^2 = A_1 + \frac{(A_2 + A_3(T - A_8)(T + A_9))}{\lambda^2 - (A_4 - A_5(T - A_8)(T + A_9)^2)} + A_6(T - A_8)(T + A_9) - A_7\lambda^2.$$

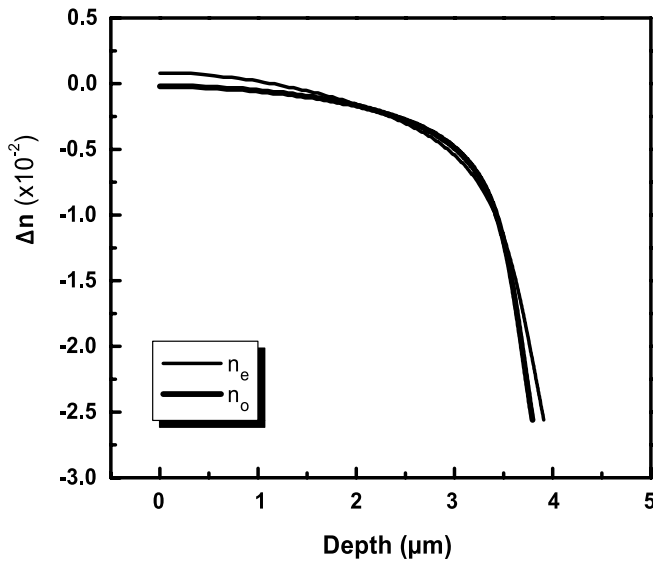


FIGURE 1 Refractive-index profiles of triple He<sup>+</sup>-implanted PPZnLN planar waveguide

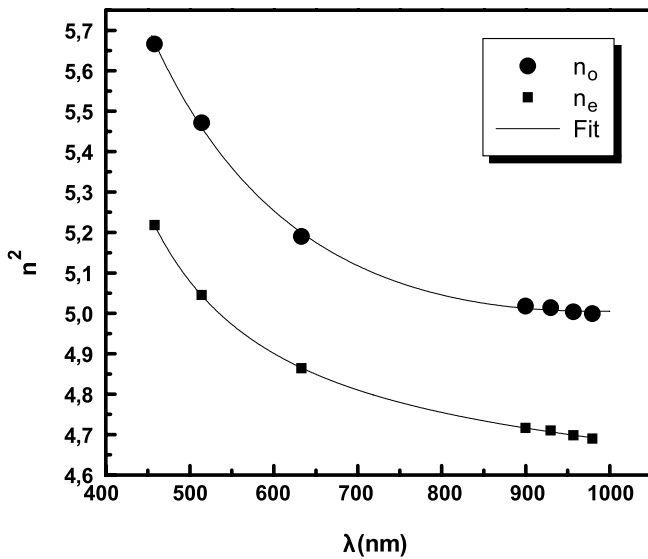


FIGURE 2 Refractive indices ( $n_o$  and  $n_e$ ) of He<sup>+</sup>-implanted PPZnLN waveguide vs. wavelength

Here,  $\lambda$  is the wavelength,  $T$  is the temperature and  $A_i$  are Sellmeier coefficients.

The best values of those coefficients are reported in Table 1. This equation can be extrapolated to a small extent; indeed, it is valid only out of the absorption region and it diverges with short wavelengths. Nevertheless, this equation enables us to make theoretical calculations of quasi-phase-matching wavelengths related to the second harmonic interaction type which occurs within the guide.

The optical loss measurements were performed by using prism in-coupling and end-fire out-decoupling as described in [34, 35]. For instance, we present in Fig. 3 the optical loss measurements carried out at  $\lambda = 514$  nm for different TM guided mode orders. It is seen that the optical losses increase rapidly with the mode number due very likely to the tunneling effect, which is dominant for higher-order modes.

Coeff.	$n_o$	$n_e$
$A_1$	5.1	4.6
$A_2$	220430	90695
$A_3$	-0.078	0.95
$A_4$	0.056	205.1
$A_5$	$-5.7 \times 10^{-7}$	0.0046
$A_6$	$5.6 \times 10^{-6}$	-2.6
$A_7$	$-2.5 \times 10^{-7}$	4.4
$A_8$	57.2	13.4
$A_9$	2640	2548.2

TABLE 1 Sellmeier coefficients of implanted PPZnLN waveguide (room temperature)

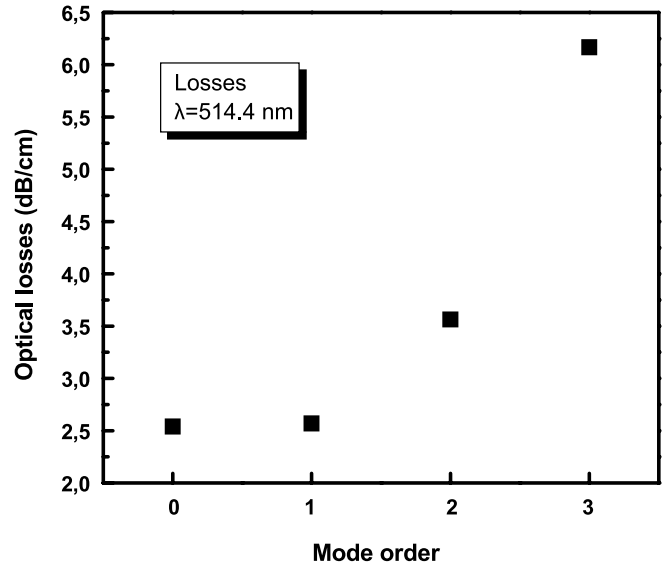


FIGURE 3 Optical losses as a function of the guided mode order. He<sup>+</sup>-implanted PPZnLN planar waveguide

In other respects, it is well established that optical losses in implanted waveguides have three origins [36, 37]: diffusion, absorption and the optical tunneling effect. As ionic implantation generally creates electronic and nuclear defects within the guide, the optical absorption of that area might slightly increase, particularly for short wavelengths. Losses by diffusion also increase when the wavelengths decrease because of Rayleigh diffusion (defects of  $\sim 10$  nm in diameter) that is proportional to  $\lambda^{-4}$ . Lastly, losses by the optical tunneling effect remain the principal problem encountered in waveguides fabricated by ionic implantation. These losses increase with the mode order and with the wavelength, as well (in contrast to the other contributions previously mentioned). The higher the wavelength, the more the electric field extends in the vicinity of the optical barrier. Pliska et al. [36, 37] showed that those losses vary as  $\lambda^6$ . Although these losses can be substantially reduced by broadening the optical barrier obtained by multiple implantations, they are no less prejudicial to the good quality of the obtained waveguides.

From that perspective, we measured the optical losses according to the wavelength. Table 2 presents a summary of the obtained results. It seems that losses for the zero-order modes are higher at short wavelengths. The general behavior of optical losses vs. wavelength is similar to that already reported by Pliska et al. in KNbO<sub>3</sub>-implanted waveguides [36, 37]. In

$\lambda$ (nm)	$m$ (TM mode order)			
	0	1	2	3
514.4	2.5	2.6	3.6	6.2
633	1.7	2.2	2.7	–
820	2.1	3	3.5	–

**TABLE 2** Optical losses in He<sup>+</sup>-implanted PPZnLN waveguide ( $\pm 0.2$  dB/cm)

other words, at short wavelengths diffusion is dominant with a variation proportional to  $\lambda^{-4}$  and at higher wavelengths tunneling becomes dominant with a variation shape of  $\lambda^6$ .

Finally, losses measured on this sample remain important, after all. However, one has to point out that the sample did not undergo any additional heat treatment and the guide parameters are not optimum. The optimization of the optical barrier parameters should enable us to reduce the losses towards more acceptable levels, i.e. below 1 dB/cm [30].

### 3.2 Investigation of second-harmonic generation

In Sect. 3.1, we have stated that the utilization of a Zn-doped LN crystal does not modify (except obviously for the refractive indices) the conditions of waveguide fabrication. The principal motivation of our work being the study of the influence of doping by zinc on the nonlinear properties of the implanted guides of periodically poled lithium niobate, we must show for the first time that it is possible to obtain second-harmonic generation in this type of PPZnLN:He<sup>+</sup> waveguide.

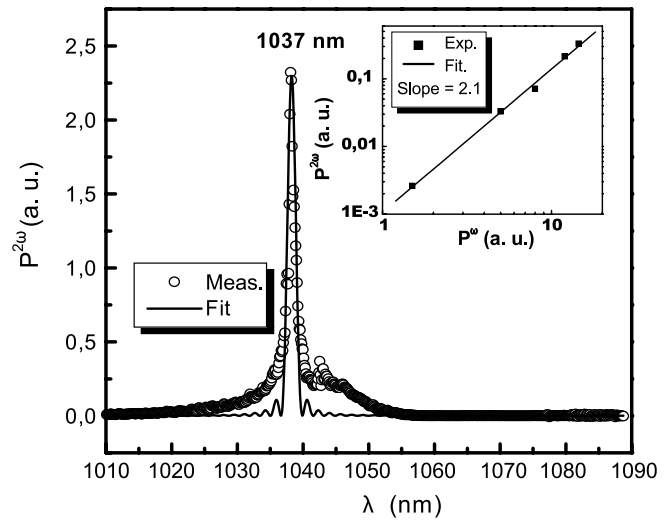
The experimental set-up used for the study of SHG is basically a pump source (Ti:sapphire or Nd:YAG laser) coupled into and out of the guide through two microscope objectives monitored by a mechanical system to ensure a maximum power to be launched into the guide. An infrared filter is used just in front of a photodetector to collect the harmonic signal generated by the SHG process and a set of neutral density filters allows the control of the pump power at the entrance of the waveguide.

Figure 4 shows the variation of the harmonic power according to the fundamental wavelength. This curve was fitted by the following classical relation:

$$P^{2\omega} \propto \left[ \frac{\sin(\Delta kd/2)}{\Delta kd/2} \right]^2 \quad (\alpha : \text{proportional}),$$

where  $\Delta k$  is the difference between the wave vectors for the fundamental and the harmonic waves and  $d$  is the interaction length.

The peak of the first-order quasi-phase matching is observed at 1037 nm. The asymmetry of the peak can be due to inhomogeneity of the waveguide as already reported by other authors [37, 38]. The inset in Fig. 4 shows the harmonic power



**FIGURE 4** Second-harmonic intensity as a function of the fundamental wavelength for He<sup>+</sup>-implanted PPZnLN planar waveguide. Inset: the SH signal vs. the fundamental power

according to the fundamental power. It is noted that the slope coefficient of 2.1 confirms the second-order process.

A rather good agreement is obtained between the theoretical and the experimental quasi-phase-matching wavelengths as indicated in Table 3. The SHG process is found to be a  $TM_0^\omega \Rightarrow TM_0^{2\omega}$  conversion. The deduced interaction length is about 1.3 mm. This value differs from the real sample length, indicating that the PPZnLN grating is not homogeneous throughout the entire sample length as has been seen by a direct observation of the grating through an optical microscope. The conversion efficiency was found to be  $10^{-2}\%$ /W. These results are far from the objectives that we fixed but, nevertheless, they constitute a first step towards a thorough study in order to improve the performance of frequency doubling in our guides, in particular by using channel waveguides. Finally, the temperature tuning curves of SHG showed a maximum green-peak power of 100  $\mu$ W for 250 mW of fundamental pump. These results show that the nonlinearity and the periodic grating remain in the guiding region after implantation.

After this study, we were interested in the photorefractive effect in those guides. For that, and in accordance with a similar study of Peng et al. [20] on bulk PPZnLN crystals, we carried out a comparative study of second-harmonic generation with various powers, by analyzing the relative intensity of the harmonic signal (HS) according to time in implanted waveguides (under the same conditions) of Zn-doped and undoped PPLN crystals.

Results are reported in Fig. 5. We can see that for an excitation of 250 mW the intensity of the SH signal is stable in PPZnLN:He<sup>+</sup>, whereas it strongly decreases in time in undoped PPLN:He<sup>+</sup>. Note that the two waveguides are similar.

Bulk PPLN:Zn $\lambda_{\text{QPM}}$ (nm)		SHG – PPLN:Zn waveguide		
Theory	Exp.	Interaction $TM_0(\omega) \rightarrow TM_0(2\omega)$	$I_{\text{OVL}}$ ( $\text{m}^{-1/2}$ )	$\lambda_{\text{QPM}}$ (nm)
1057	1039		1296	1067
				$\lambda_{\text{QPM}}$ (nm) 1037

**TABLE 3** Summary of SHG results in PPZnLN bulk crystals and He<sup>+</sup>-implanted waveguide

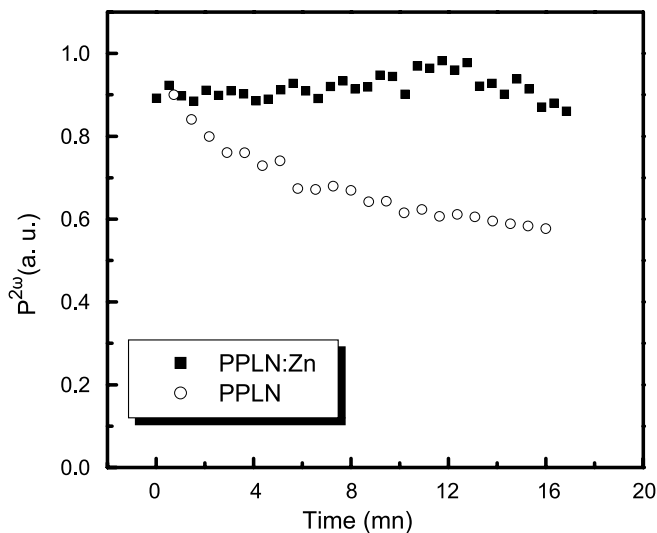


FIGURE 5 Variation of SH signal vs. time for He<sup>+</sup>-implanted PPZnLN and He<sup>+</sup>-implanted un-doped PPLN waveguides

They have been fabricated in exactly the same conditions. The injection of the pump power has also been performed in the same experimental conditions. Therefore, one can consider that both experiments have been conducted with the same power density.

This result indicates that the initial resistance to the photorefractive effect of Zn-doped crystal is well preserved in the implanted waveguide. Therefore, the implantation does not modify (or only a little) the intrinsic properties of the crystal. This last result is of very great importance because it emphasizes the interest of implanted waveguides in Zn-doped PPLN.

#### 4 Conclusion

We investigated the optical linear and nonlinear properties of planar waveguides fabricated in PPZnLN crystals by using triple implantation of He<sup>+</sup> ions. Without any additional heat treatment of the sample, optical losses were found to be about 2 dB/cm. This value is similar to those reported in LiNbO<sub>3</sub>-implanted waveguides. We focused on the study of resistance to optical damage by measuring the SH intensity related to operation time of the device. Results indicated a good stability of the SH signal over 20 min. This result is of great importance because it shows that the combination of light-ion implantation with Zn-doped PPLN structures might allow us to clear up a major problem encountered in developing compact miniature laser sources emitting at short wavelengths, namely resistance to optical damage and lifetime limitations.

#### REFERENCES

- 1 F. Laurell, *Opt. Mater.* **11**, 235 (1999)
- 2 J. Webjörn, S. Siala, W. Nam, R.G. Waarts, R.L. Lang, *IEEE J. Quantum Electron.* **QE-10**, 1673 (1997)
- 3 S. Greenstein, M. Rosenbluh, *Opt. Commun.* **238**, 319 (2004)
- 4 S.E. Kapphan, *J. Luminesc.* **83-84**, 411 (1999)
- 5 A. Ashkin, D.D. Boyd, J.M. Dziedzic, R.G. Smith, A.A. Ballman, J.J. Levinstein, K. Nassau, *Appl. Phys. Lett.* **9**, 72 (1966)
- 6 P. Günther, J.-P. Huignard, *Photorefractive Materials and Their Applications I* Top. Appl. Phys., Vol. 61 (Springer, Berlin, 1988)
- 7 A.M. Prokhorov, Y.S. Kuz'minov, *Physics and Chemistry of Crystalline Lithium Niobate* (Adam Hilger, Bristol, 1990)
- 8 B.I. Sturman, V.M. Fridkin, *The Photovoltaic and Photorefractive Effects in Noncentrosymmetric Materials* (Gordon and Breach, Reading, UK, 1992)
- 9 V. Pruneri, P.G. Kazansky, J. Webjörn, P.S.J. Russell, D.C. Hanna, *Appl. Phys. Lett.* **67**, 1957 (1995)
- 10 I. Nee, M. Müller, K. Buse, E. Krätzig, *J. Appl. Phys.* **88**, 4282 (2000)
- 11 D. Fluck, S. Brülisauer, P. Günter, C. Buchal, L. Beckers, *Nucl. Instrum. Methods Phys. Res. B* **148**, 678 (1999)
- 12 B. Sturman, M. Aguilar, F.A. Lopez, V. Pruneri, P.G. Kazansky, D.C. Hanna, *Appl. Phys. Lett.* **69**, 1349 (1996)
- 13 D.A. Bryan, R. Gerson, H.E. Tomaschke, *Appl. Phys. Lett.* **44**, 847 (1984)
- 14 A. Ballman, *J. Am. Ceram. Soc.* **48**, 112 (1965)
- 15 K. Polgár, Á. Péter, L. Kovács, G. Corradi, Z. Szaller, *J. Cryst. Growth* **177**, 211 (1997)
- 16 Y. Furukawa, K. Kitamura, S. Takekawa, K. Niwa, H. Hatano, *Opt. Lett.* **23**, 1892 (1998)
- 17 Y. Kong, J. Xu, X. Chen, C. Zhang, W. Zhang, G. Zhang, *J. Appl. Phys.* **87**, 4410 (2000)
- 18 V.Y. Shur, E.L. Rumyantsev, R.V. Nikolaeva, E.I. Shishkin, R.G. Batchko, M.M. Fejer, R.L. Byer, *Ferroelectrics* **257**, 191 (2001)
- 19 T.R. Volk, V.I. Pryalkin, N.M. Rubina, *Opt. Lett.* **15**, 996 (1990)
- 20 L.H. Peng, Y.-C. Zhang, Y.-C. Lin, *Appl. Phys. Lett.* **78**, 4 (2001)
- 21 P.D. Townsend, P.J. Chandler, L. Zhang, *Optical Effects of Ion Implantation* (Cambridge University Press, Cambridge, UK, 1994)
- 22 A. Boudrioua, F. Laurell, P. Moretti, J.C. Loulergue, *J. Opt. Soc. Am. B* **18**, 1832 (2001)
- 23 B. Vincent, A. Boudrioua, R. Kremer, P. Moretti, *Opt. Commun.* **247**, 461 (2005)
- 24 N. Towghi, B. Javidi, Z. Lou, *J. Opt. Soc. Am. B* **16**, 1915 (1999)
- 25 P. Mathey, A. Dazzi, P. Jullien, D. Rytz, P. Moretti, *J. Opt. Soc. Am. B* **18**, 344 (2001)
- 26 A. Dazzi, P. Mathey, P. Lompre, P. Jullien, S.G. Odoulov, *J. Opt. Soc. Am. B* **16**, 256 (1999)
- 27 M. Houé, P.D. Townsend, *J. Phys. D Appl. Phys.* **28**, 1747 (1995)
- 28 G.D. Miller, Ph.D. thesis, Stanford University, USA, 1998
- 29 L.E. Myers, R.C. Eckardt, M.M. Fejer, R.L. Byer, W.R. Bosenberg, J.W. Pierce, *J. Opt. Soc. Am. B* **11**, 2102 (1995)
- 30 A. Dazzi, P. Mathey, P. Lompre, P. Jullien, *Opt. Commun.* **149**, 135 (1998)
- 31 R. Ulrich, R. Torge, *Appl. Opt.* **12**, 2901 (1973)
- 32 K.S. Chiang, *J. Lightwave Technol.* **LT-3**, 385 (1985)
- 33 P. Mathey, P. Jullien, J.L. Bolzinger, *J. Opt. Soc. Am. B* **12**, 1663 (1995)
- 34 A. Boudrioua, J.C. Loulergue, *Opt. Commun.* **137**, 37 (1997)
- 35 A. Boudrioua, C. Bakhouya, J.C. Loulergue, P. Moretti, K. Polgar, *J. Appl. Phys.* **89**, 7716 (2001)
- 36 T. Pliska, D. Fluck, P. Günter, L. Beckers, C. Buchal, *J. Opt. Soc. Am. B* **2**, 628 (1998)
- 37 T. Pliska, D. Fluck, P. Günter, L. Beckers, C. Buchal, *J. Appl. Phys.* **3**, 1186 (1998)
- 38 A. Boudrioua, J.C. Loulergue, P. Moretti, B. Jacquier, G. Aka, D. Vivien, *Opt. Lett.* **24**, 1299 (1999)